European Radiology (2019) 29:2507–2517
https://doi.org/10.1007/s00330-018-5839-7

UROGENITAL

Evaluation of a free-breathing respiratory-triggered (Navigator) 3-D T1-weighted (T1W) gradient recalled echo sequence (LAVA) for detection of enhancement in cystic and solid renal masses

Wendy Tu[1] · Abdulrahman Alzahrani[1] · Stephen Currin[1] · Cindy Walsh[1] · Sabarish Narayanasamy[1] · Matthew D. F. McInnes[1] · Nicola Schieda[1]

Received: 22 May 2018 / Revised: 15 September 2018 / Accepted: 17 October 2018 / Published online: 30 November 2018

Abstract

Objectives To evaluate free-breathing Navigator-triggered 3-D T1-weighted MRI (NAV-LAVA) compared to breath-hold (BH)-LAVA among cystic and solid renal masses.

Materials and methods With an IRB waiver, 44 patients with 105 renal masses (71 non-enhancing cysts and 14 cystic and 20 solid renal masses) underwent MRI between 2016 and 2017 where BH-LAVA and NAV-LAVA were performed. Subtraction images were generated for BH-LAVA and NAV-LAVA using pre- and 3-min post-gadolinium-enhanced images and were evaluated by two blinded radiologists for overall image quality, image sharpness, motion artifact, and quality of subtraction (using 5-point Likert scales) and presence/absence of enhancement. Percentage signal intensity change (Δ%SI) = ([SI.post-gadolinium-SI.pre-gadolinium]/SI.pre-gadolinium)*100, was measured on BH-LAVA and NAV-LAVA. Likert scores were compared using Wilcoxon's sign-rank test and accuracy for detection of enhancement compared using receiver operator characteristic (ROC) analysis.

Results Overall image quality ($p = 0.002$–0.141), image sharpness ($p = 0.002$–0.031), and motion artifact were better ($p = 0.002$) comparing BH-LAVA to NAV-LAVA for both radiologists; however, quality of image subtraction did not differ between groups ($p = 0.09$–0.14). Sensitivity/specificity/area under ROC curve for enhancement in cystic and solid renal masses using subtraction and %SIΔ were (1) BH-LAVA: 64.7%/98.6%/0.82 (radiologist 1), 61.8%/95.8%/0.79 (radiologist 2), and 70.6%/81.7%/0.76 (%SIΔ) versus 2) NAV-LAVA: 58.8%/95.8%/0.79 (radiologist 1, $p = 0.16$), 58.8%/88.7%/0.73 (radiologist 2, $p = 0.37$), and 73.5%/76.1%/0.75 (%SIΔ, $p = 0.74$).

Conclusions NAV-LAVA showed similar quality of subtraction and ability to detect enhancement compared to BH-LAVA in renal masses albeit with lower image quality, image sharpness, and increased motion artifact. NAV-LAVA may be considered in renal MRI for patients where BH is suboptimal.

Key Points

- *Free-breathing Navigator (NAV) 3-D subtraction MRI is comparable to breath-hold (BH) images.*
- *Accuracy for subjective and quantitative diagnosis of enhancement in renal masses on NAV 3-D T1W is comparable to BH MRI.*
- *NAV 3-D T1W renal MRI is useful in patients who may not be able to adequately BH.*

Keywords Magnetic resonance imaging · Kidney · Neoplasms · Renal cell carcinoma · Image enhancement

Abbreviations

% SI Change	Percentage of signal intensity difference
AMLs	Angiomyolipomas
BH-LAVA	Breath-hold 3-D T1-weighted MRI
BH	Breath-hold
FS	Fat-suppressed
FSE	Fast spin echo
GRE	Gradient recalled echo
HU	Hounsfield units
IgG4	Immunoglobulin G4-related disease
LAVA	Gradient recalled echo sequence
NAV-LAVA	Navigator-triggered 3-D T1-weighted MRI
NAV	Free-breathing Navigator
PACS	Picture archiving and communication system
RCC	Renal cell carcinoma

✉ Nicola Schieda
nschieda@toh.on.ca

[1] The Ottawa Hospital, The University of Ottawa, 1053 Carling Avenue, Ottawa, Ontario K1Y 4E9, Canada

ReKAM	Repeated K-t-subsampling and artifact-minimization
ROI	Region of interest
T1W	T1-weighted MRI
T2W	T2-weighted MRI
VIBE	Volumetric interpolated breath-hold examination

Introduction

Indeterminate renal masses are common [1], and although CT remains the mainstay for renal mass characterization [2], MRI provides comparable and, in some instances, additional information [3]. Among hyperattenuating renal masses, characterization of internal contents with MRI is better than with CT [4–6]. MRI assessment of enhancement is more sensitive than CT in papillary renal cell carcinoma (RCC) [7, 8] and more specific due to elimination of pseudoenhancement [2, 4, 7, 9, 10]. MRI is accurate for subtyping small solid renal masses [3, 11–14]. Willatt et al showed that renal MRI provided additional diagnostic information in a majority of small renal masses which were indeterminate on CT [15].

One of the fundamental requirements of renal MRI is high-quality pre- and post-gadolinium-enhanced images, which form the basis for diagnosis of enhancement [16].

Enhancement may be assessed by measuring the percentage of signal intensity difference (%SI. change) [17] or by qualitative assessment of subtraction images generated by withdrawing pre-gadolinium-enhanced data from post-gadolinium-enhanced data where the difference is displayed visually and is indicative of enhancement [18]. Subtraction images are routinely used in renal MRI and are invaluable for the assessment of inherently T1-weighted (T1W) hyperintense masses [4, 9]. In a study by Hecht et al, qualitative assessment of subtraction images was comparable to quantitative analysis and less prone to errors among intrinsically T1W hyperintense masses [18]. A limitation of subtraction MRI is the requirement for perfectly co-registered data because any malalignment between image sets can result in interpretive errors [3, 9]. End-expiratory phase breath-hold imaging improves co-registration of pre- and post-gadolinium-enhanced image sets [3, 4]; however, subtraction imaging may still be limited in patients who cannot suspend respiration consistently.

The use of free-breathing T1W gadolinium-enhanced imaging has traditionally been limited by severe motion artifacts; however, more recently, vendors have provided commercially available solutions to improve image quality. Gadolinium-enhanced images may be acquired free-breathing when the acquisition is timed to coincide with end-tidal expiration using a simultaneously acquired Navigator acquisition tracking motion of the diaphragm (Navigator LAVA, General Electric Company) or by using a radial stack-of-stars sampling of k-space (Star-VIBE Siemens Healthcare) [19]. Studies have shown that both techniques are robust against motion artifact in the abdomen [19, 20]; however, to our knowledge, neither technique has been studied as an alternative to obtain subtraction images in renal MRI. The purpose of this study is therefore to compare free-breathing Navigator (NAV) T1W and breath-hold (BH) T1W subtraction images in patients undergoing renal MRI.

Materials and methods

Patients

This retrospective study was performed under a quality assurance waiver from our institutional review board who waived the need for informed consent in patients. Between the dates of April 2016 and February 2017, 77 patients underwent renal MRI at a single institution which included pre- and post-gadolinium-enhanced images acquired using end-expiratory phase BH and NAV acquisitions. From 77 patients, 33 were eventually excluded with a summary of the patient inclusion and exclusion criteria provided in Fig. 1.

Renal lesions and reference standards

From 44 patients who met the inclusion criteria, there were 71 non-enhancing benign renal cysts (46 simple cysts and 25 hyperattenuating or hemorrhagic/proteinaceous cysts) and 34 cystic or solid renal masses (9 Bosniak 2F renal cysts, 5 Bosniak 3 renal cysts, 18 solid enhancing renal masses [6 histologically confirmed RCC] and two > 1-cm AMLs). Mean size of lesions was 21 mm (± 13; range of 10–80). The reference standards used for diagnosis of non-histologically confirmed renal masses is described as follows: (1) benign renal cysts—round or oval, smooth paper thin wall, homogeneously hyperintense on T2-weighted (T2W) and hypointense on T1W imaging without enhancement on subtraction images [4] and with either unenhanced CT showing round or oval shape, smooth imperceptible wall and homogeneous water (-10 to < 20 Hounsfield Units [HU]) attenuation [21] or ultrasound showing homogeneously anechoic structure with smooth imperceptible wall and increased through transmission [10]; (2) hyperattenuating cysts—round or oval, homogeneously markedly T1W hyperintense [22, 23] without enhancement on subtraction images [4] and with either unenhanced CT showing > 70 HU [24] or ultrasound showing homogeneously anechoic structure or with few low level echoes with smooth imperceptible wall and increased through transmission [10]; (3) Bosniak 2F or 3 cysts—T2W hyperintense lesion with low T2W internal septations showing enhancement on subtraction images [25] and with multiphase CT showing perceptible enhancement of thin septations (for Bosniak 2F) and measurable enhancement of thicker septations (for Bosniak 3) [6]; (4) solid enhancing lesion without

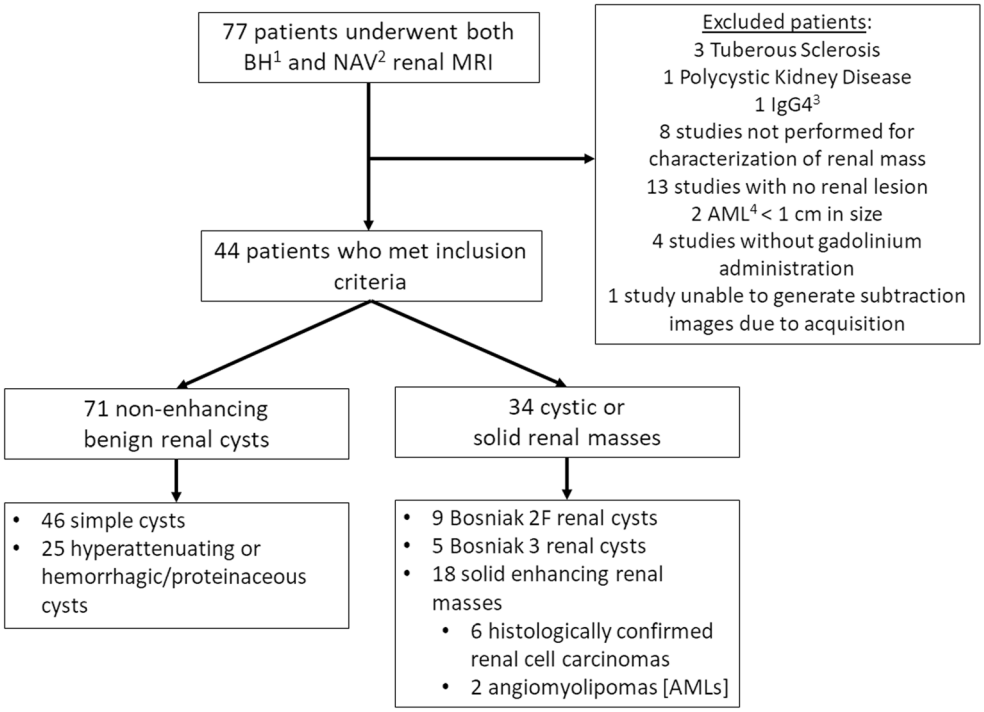

Fig. 1 Flow diagram of patient inclusion and exclusion in this study. 1 = breath-hold, 2 = navigator-triggered free-breathing, 3 = IgG4-related systemic disease, 4 = angiomyolipoma

histological confirmation—non-cystic mass on MRI with > 80% enhancing components on subtraction imaging and with multiphase CT showing enhancement of at least 25 HU in > 80% of the mass [4]; and (5) angiomyolipoma—a mass showing internal macroscopic or bulk fat as determined by area of fat showing signal loss using chemical fat suppression and attenuation measurements at unenhanced CT < -20 HU [26, 27]. Imaging-based reference standards were determined by an unblinded abdominal radiology fellow and genitourinary radiologist with 11 years of experience in renal CT and MRI (NS) who had access to all prior ultrasound, CT, and MRI reports.

MRI

All patients underwent MRI on a clinical 3-Tesla MRI (Discovery 750 W, General Electric Healthcare) using integrated body surface (16-element) array and spine coils. Our renal mass MRI protocol consists of BH axial and coronal T2W single-shot fast spin echo (FSE), BH axial 3-dimensional (3-D) T1W in- and opposed-phase dual-echo chemical shift gradient recalled echo (GRE), BH axial fat-suppressed (FS) diffusion-weighted echo-planar imaging and BH axial pre-and post-gadolinium FS T1W 3-D GRE (LAVA) sequences with 5-min delayed axial and coronal acquisitions. Post-gadolinium-enhanced images were acquired dynamically after the administration of 0.1 mmol/kg of gadobutrol (Gadovist, Bayer Healthcare) injected at a rate of 2 mL/s followed by 20 mL saline flush. Axial BH post-gadolinium-enhanced images were obtained following an empiric 30–40 s delay followed by successive acquisitions every minute for 3–5 min. The first axial BH T1W LAVA sequence (obtained at 30–40 s) was used as the corticomedullary phase and the third axial BH T1W LAVA sequence (obtained at 60–80 s) was used as the nephrographic phase. For the pre- and post-gadolinium-enhanced T1W BH-LAVA sequences, all breath-holds are performed at end-tidal expiration. Subtraction image sets are generated for the corticomedullary phase, nephrographic phase, and 3-min delayed acquisitions routinely and stored in our PACS (Horizon Medical Imaging version 11.1, McKesson Corporation).

Throughout the study period, all patients also underwent free-breathing NAV FS 3-D T1W LAVA before gadolinium injection (immediately following the breath-hold FS 3-D T1W LAVA sequence) and after gadolinium injection (immediately following the 3-min breath-hold FS 3-D T1W LAVA acquisition). Therefore, all patients underwent BH and NAV T1W LAVA before and approximately 3 min after gadolinium injection. The details of the Navigator LAVA sequence have been described in detail elsewhere [28]. To reduce acquisition time such that the examinations were not significantly prolonged, an acceleration factor of 3 in the phase direction and 2 in the slice direction of the Navigator LAVA sequence was applied. Further details regarding the BH and Navigator LAVA are summarized in Table 1. A larger field of view was selected for the NAV sequence to mitigate the loss of signal to noise incurred by increased parallel imaging utilized on NAV compared to BH and also to reduce parallel imaging (i.e., sense ghosting or aliasing) artifacts from signal contributions outside of the region of interest. Subtraction images were obtained for the Navigator LAVA sequence using AquariusNet version 11 (TeraRecon corporation) and also stored in PACS.

Table 1 Pulse sequence parameters for conventional breath-hold and free-breathing Navigator-triggered T1-weighted Fat-Suppressed 3-D gradient recalled echo with volume acceleration (LAVA)

Parameter	Breath-hold	Navigator
TR[1] (ms)	3.9	4.4
TE[2] (ms)	1.7	1.9
Matrix	224 × 320	192 × 300
Field of view (cm)	352 × 440	460 × 460
Slice thickness (mm)	4	4
Gap (mm)	2	2
Flip angle	12	12
Fat suppression	Spectral + inversion recovery	Spectral + inversion recovery
NEX[3]	0.67	0.70
Acceleration	Phase 2 slice 1	Phase 3 slice 2
Bandwidth (KHz)	83.3	62.5
Acquisition time (s)	18	150

Breath-hold was performed during end-tidal expiration

[1] Time to repetition

[2] Time to echo

[3] Partial Fourier factors

Subjective analysis

Subjective analysis was performed by two Radiologists with 5 and 14 years of experience with renal MRI (SC and CW). Each examination was evaluated in two interpretation sessions (time between interpretation sessions of 10 weeks for radiologist 1 and 8 weeks for radiologist 2) using a mixed-order readout fashion to minimize bias. Examinations were evaluated independently. Radiologists could not be blinded to whether BH or NAV imaging was being interpreted due to the predictable periodic motion of the abdominal wall which could be observed during NAV imaging (Figs. 2, 3, and 4); however, they were blinded to the final diagnosis of each lesion.

Image quality

Radiologists were provided with a brief lecture and presentation describing which imaging quality features were to be evaluated for each examination before beginning data extraction (Figs. 2, 3, and 4). Before data extraction, radiologists were provided with the location of each lesion which needed to be assessed. Radiologists subjectively assessed BH and NAV image sets for (1) overall image quality: subjective evaluation of the kidneys and the lesion(s) being evaluated, judged using a 5-point Likert scale where 1 = non-diagnostic, 2 = below average or poor, 3 = average, 4 = above average or good, and 5 = excellent; (2) image sharpness: subjective evaluation of the edges or interfaces between the kidney borders and the retroperitoneal fat, renal sinus, and borders of the lesion(s) being assessed judged using a 5-point Likert scale where 1 = non-diagnostic, 2 = below average or poor, 3 = average, 4 = above average or good, and 5 = excellent; and (3) motion artifact: subjective evaluation of degree of periodic or random motion (ringing, blurring, smearing, or ghosting of structures) of the kidneys and lesion(s) being assessed judged using a 5-point Likert scale where 1 = no motion artifact, 2 = minimal motion which does not impact evaluation of the kidneys or renal lesions, 3 = mild motion artifact compromising image quality but with a diagnostic assessment still achieved, 4 = moderate motion artifact impacting evaluation of the renal lesion(s), and 5 = severe motion with non-diagnostic assessment. In addition, both radiologists evaluated subtraction image sets using a 5-point Likert scale for quality of image subtraction where 1 = non-diagnostic, 2 = below average or poor, 3 = average, 4 = above average or good, and 5 = excellent. The use of 5-point Likert scales for comparison of MR imaging sequences has been described previously [29, 30].

Enhancement

Both radiologists independently assessed each lesion for the presence of either septal or solid enhancement using subtraction images only. Radiologists did not evaluate the other pre-contrast images (including T1W and T2W sequences) or the raw data from the pre- and post-gadolinium-enhanced LAVA sequences when judging for the presence of enhancement. This study design was selected in order to enable the most robust and unbiased comparison of the accuracy of enhancement using subtraction images derived from BH and NAV sequences. Enhancement was defined as being present when there was unequivocally an increase in signal within the renal lesion as judged on subtraction images and was scored using a binary outcome where 1 = present and 2 = absent (Figs. 2, 3, and 4), as described previously [18].

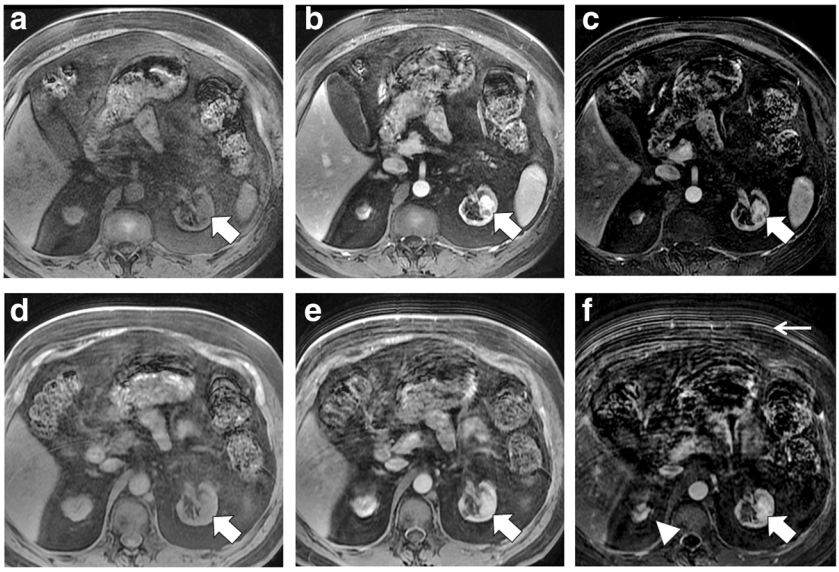

Fig. 2 A 55-year-old male patient with left upper pole clear cell renal cell carcinoma (RCC). Axial fat- suppressed breath-hold (BH) T1-weighted (T1W) 3-D LAVA images obtained before (**a**) and after (**b**) gadolinium enhancement in the nephrographic phase show solid enhancement in the tumor which is located within the left renal hilum (arrows). Subtraction (**b** minus **a**) image (**c**) clearly depicts enhancement in the mass. Image quality, image sharpness, and quality of subtraction were rated 5/5 by both radiologists. Free-breathing Navigator-triggered (NAV) LAVA images at the same level obtained before (**d**) and after (**e**) gadolinium enhancement in the nephrographic phase also show solid enhancement in the tumor (arrows) which is confirmed in corresponding subtraction image (**f**) Image quality and quality of subtraction were rated 5/5 by both radiologists. Image sharpness was considered average (3/5) by both radiologists with some blurring of the renal margins best depicted in the upper pole of the right kidney (arrowhead in **f**) with motion artifacts (thin white arrow in **f**) from the anterior abdominal wall which were considered to not compromise diagnostic accuracy of the study

Quantitative analysis

Ten weeks following the second interpretation session, radiologist 1 independently measured signal intensity values on BH and NAV pre- and 3-min post-gadolinium-enhanced LAVA sequences. A circular region of interest (ROI) was placed within the center of the lesion on the axial image where it appeared the largest encompassing two thirds of the area of

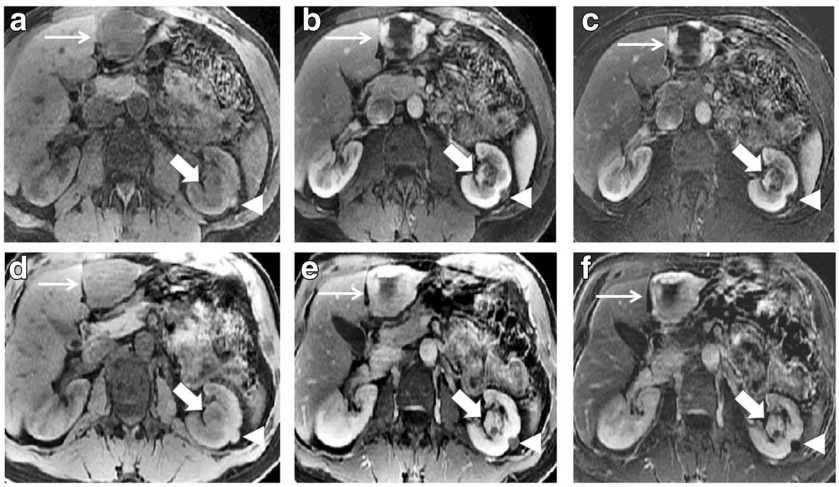

Fig. 3 A 62-year-old female patient with left hilar clear cell RCC. Axial BH 3-D LAVA images obtained before (**a**) and after (**b**) gadolinium enhancement in the nephrographic phase show areas of solid enhancement in the tumor which also shows small cystic spaces in the left renal hilum (arrows). Subtraction (**b** minus **a**) image (**c**) clearly depicts enhancement in the mass. There is another 12-mm lesion in the interpolar region lateral cortex (arrowheads) which was proven to represent a complex hemorrhagic/proteinaceous cyst at subsequent ultrasound exam (not shown). The cyst is intrinsically T1W hyperintense in (**a**) and non-enhancing on subtraction image (**c**); however, the contours of the cyst are blurred by motion artifact and motion and image sharpness were both rated as 3/5 by both radiologists. Corresponding NAV-LAVA images at the same level obtained before (**d**) and after (**e**) gadolinium enhancement in the nephrographic phase also show solid enhancement in the tumor (arrows) which is confirmed in corresponding subtraction image (**f**) and better depict the hemorrhagic/proteinaceous cyst (arrowheads). Image sharpness and degree of motion artifact were considered better in this patient on NAV-LAVA compared to BH-LAVA by both radiologists. Also note benign hepatic hemangioma in the lateral segment (thin arrows)

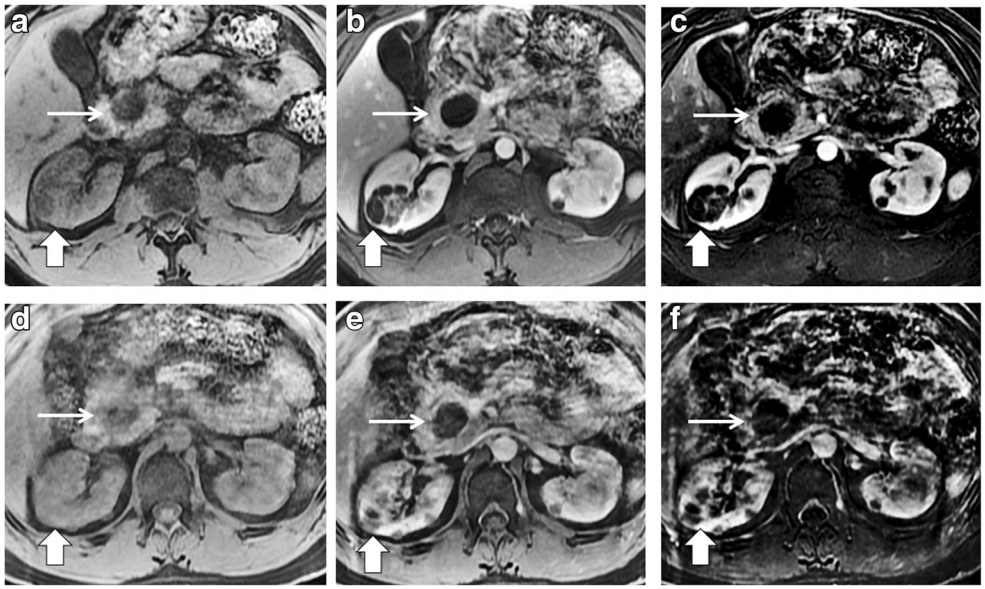

Fig. 4 A 45-year-old female patient with right interpolar region Bosniak III cystic mass. Axial BH-LAVA images obtained before (**a**) and after (**b**) gadolinium enhancement in the nephrographic phase show thick septal enhancement with areas of measurable enhancement in the tumor which is located within the renal hilum (arrows). Subtraction image (**c**) clearly depicts enhancement in the mass. Image quality, image sharpness, and quality of subtraction were rated 5/5 by both radiologists. Corresponding NAV-LAVA images at the same level obtained before (**d**) and after (**e**) gadolinium enhancement in the nephrographic phase also show enhancement in the tumor (arrows) which is confirmed in corresponding subtraction image (**f**); however, in this patient, image quality, image sharpness, quality of subtraction, and motion artifacts were judged to be worse on NAV-LAVA compared to BH-LAVA but did not compromise diagnostic accuracy of the study according to both radiologists. Note unilocular cystic mass in the pancreatic head (thin white arrows) which was presumed to represent a pancreatic pseudocyst or non-aggressive side-branch intraductal mucinous neoplasm

the lesion for homogeneous lesions as described previously [17, 18]. For heterogeneous lesions, an ROI was placed over the area which appeared to show the most enhancement on the post-gadolinium-enhanced image and copied to the pre-gadolinium-enhanced data set, as described previously [17, 18]. Using pre- and post-gadolinium-enhanced signal intensity values, a percentage of signal intensity change was calculated as follows: ([signal intensity on post-gadolinium image minus signal intensity on pre-gadolinium image] / signal intensity on pre-gadolinium image) * 100% [17, 18]. A signal intensity change of > 15% was used to define enhancement [17, 18]. The ROI was copy-pasted such that it was placed at the same location on BH and NAV images for each patient.

Statistical analysis

Data are reported as mean ± standard deviation (range). Comparisons of image quality scores were performed using the Wilcoxon sign-rank test. Accuracy of enhancement judged subjectively was calculated for subtraction imaging of BH and NAV data sets for both radiologists and compared using receiver operator characteristic (ROC) analysis. Inter-observer agreement was assessed using Cohen's kappa statistic where: 0.00–0.20 is slight, 0.21–0.40 is fair, 0.41–0.60 is moderate, 0.61–0.80 is substantial, and > 0.81 is almost perfect. Percentage signal intensity change was compared between enhancing and non-enhancing lesions using independent *t* tests and agreement of measures between BH and NAV measurements was performed using Bland-Altman. Accuracy for diagnosis of enhancement using a percentage signal intensity change of > 15% was tabulated to reference standard for both BH and NAV sequences and compared using ROC. Statistical analysis was performed using STATA version 15.1 (StataCorp) and p values of < 0.05 were considered significant.

Results

Assessment of overall image quality, image sharpness, motion artifact, and quality of image subtraction are provided in Table 2. Overall image quality was rated higher for BH compared to NAV by radiologist 2 ($p = 0.002$) but with no difference as judged by radiologist 1 ($p = 0.14$). Image sharpness was rated higher with BH imaging for both radiologists ($p =$ 0.002–0.03) and the degree of motion artifact was worse with NAV ($p = 0.002$). A summary of non-diagnostic and below average or poor image scores are provided in Table 2. There were no patients with non-diagnostic image quality with NAV imaging as judged by radiologist 1 compared to only one patient with non-diagnostic image quality as judged by radiologist 2. In terms of quality of image subtraction, there was no difference comparing the two techniques for either radiologist ($p = 0.09$–0.14).

Table 2 Subjective scores for overall image quality, image sharpness, degree of motion artifact, and quality of subtraction images provided by two radiologists using standard end-expiratory phase breath-hold versus free-breathing Navigator-triggered 3-D T1W FS GRE before and after gadolinium administration

	Overall image quality		Image sharpness		Motion artifact		Quality of subtraction	
	Breath-hold	Navigator free-breathing	Breath-hold	Navigator free-breathing	Breath-hold	Navigator free-breathing	Breath-hold	Navigator free-breathing
Radiologist 1	4.0 ± 0.8 (3–5)	3.8 ± 0.7 (2–5)	4.0 ± 0.9 (2–5)	3.7 ± 0.8 (2–5)	1.7 ± 0.8 (1–4)	2.2 ± 0.8 (1–4)	4.2 ± 0.8 (2–5)	3.9 ± 0.8 (2–5)
p value[1]	0.14		0.03		0.002		0.09	
Radiologist 2	3.2 ± 0.8 (2–5)	2.6 ± 0.7 (1–4)	3.4 ± 0.9 (2–5)	2.7 ± 0.8 (1–4)	2.5 ± 0.9 (1–4)	3.0 ± 0.8 (2–5)	3.5 ± 1.1 (1–5)	3.1 ± 0.9 (1–5)
p value[1]	0.002		0.002		0.002		0.14	

[1] Comparisons were performed between groups using the Wilcoxon sign-rank test

Using only BH subtraction images, radiologist 1 correctly diagnosed no enhancement in 98.6% (70/71) and radiologist 2 95.8% (68/71) cysts, while radiologist 1 correctly diagnosed the presence of enhancement in 64.7% (22/34) and radiologist 2 61.8% (21/34) cystic or solid enhancing masses. This compares to results using only NAV subtraction images where radiologist 1 correctly diagnosed no enhancement in 95.8% (68/71) and radiologist 2 88.7% (63/71) cysts, while radiologist 1 correctly diagnosed the presence of enhancement in 58.8% (20/34) and radiologist 2 58.8% (20/34) cystic or solid enhancing masses. Sensitivity, specificity, and area under the ROC curve for detection of enhancement in benign cysts and cystic or solid renal masses using subjective analysis of subtraction imaging are provided in Table 3. There was no difference in accuracy comparing assessment of enhancement using BH or NAV subtraction images for either radiologist ($p = 0.16$–0.37).

Inter-observer agreement for detection of enhancement between radiologists using BH subtraction images was good ($K = 0.64$) and when using NAV subtraction images was moderate ($K = 0.49$). Intra-observer agreement for detection of enhancement when evaluating subtraction images using BH and NAV sequences was very good ($K = 0.81$) for radiologist 1 and moderate ($K = 0.54$) for radiologist 2.

The sensitivity, specificity, and area under the ROC curve for detection of enhancement in benign renal cysts versus cystic and solid renal masses using quantitative signal intensity percentage changes are provided in Tables 4 and 5. There was no difference in accuracy comparing detection of enhancement using quantitative analysis of BH compared to NAV imaging ($p = 0.74$). Compared to subjective analysis of subtraction images, quantitative analysis using both BH and NAV analysis showed slightly improved sensitivity but lower specificity with no difference in overall accuracy ($p = 0.51$–0.78). Mean ± standard deviation (range) percentage signal intensity change for cysts versus solid masses were BH (2.7 ± 58.1 [-43.6–46.4] versus 92.9 ± 72.4 [-12.3–234.0], $p < 0.0001$), and NAV (2.5 ± 24.0 [-64.7–73.9] versus 58.7 ± 34.8 [-13.8–129.0], $p < 0.0001$). There was excellent agreement between measurements performed on BH and NAV images with low mean difference -0.048 (CI -0.138–0.043) depicted in the Bland-Altman plot (Fig. 5).

Table 3 Subjective scores for image quality, sharpness, degree of motion artifact, and quality of subtraction images as judged by two radiologists using 5-point Likert scales on breath-hold and free-breathing Navigator-triggered 3-D T1W FS GRE in 44 consecutive patients

	Image quality	Image sharpness	Motion artifact	Quality of subtraction
Radiologist 1				
Breath-hold				
Non-diagnostic	0	0	0	0
Below average or poor	0	4.5% (2/44)	0	4.5% (2/44)
Free-breathing				
Non-diagnostic	0	0	0	0
Below average or poor	2.3% (1/44)	6.8% (3/44)	2.3% (1/44)	6.8% (3/44)
Radiologist 2				
Breath-hold				
Non-diagnostic	0	0	0	9.1% (4/44)
Below average or poor	20.5% (9/44)	20.5% (9/44)	4.5% (2/44)	4.5% (2/44)
Free-breathing				
Non-diagnostic	2.3% (1/44)	4.5% (2/44)	2.3% (1/44)	2.3% (1/44)
Below average or poor	43.2% (19/44)	36.4% (16/44)	27.3% (12/44)	22.7% (10/44)

Table 4 Sensitivity, specificity, and area under the receiver operator characteristic (ROC) curve for detection of enhancement using subjective analysis of subtraction imaging in benign renal cysts and cystic or solid renal masses

	Sensitivity (confidence intervals)	Specificity (confidence intervals)	Area under ROC curve (standard error)	*p* value[1]
Radiologist 1				
Breath-hold	64.7 (46.5–80.3)	98.6 (92.4–100.0)	0.82 (0.04)	0.16
Free-breathing navigator	58.8 (40.7–75.4)	95.8 (88.1–99.1)	0.77 (0.04)	
Radiologist 2				
Breath-hold	61.8 (43.6–77.8)	95.8 (88.1–99.1)	0.79 (0.04)	0.37
Free-breathing navigator	58.8 (40.7–75.4)	88.7 (79.0–95.0)	0.73 (0.05)	

[1] Comparisons were performed between groups using ROC statistic

Discussion

This study compared quality of imaging subtraction on pre- and post-gadolinium-enhanced T1W 3-D GRE images in cystic and solid renal masses using breath-hold and a free-breathing Navigator-triggered technique. In our study, overall image quality was better on BH compared to NAV (although the difference was significant for only one radiologist) with better image sharpness and less motion artifact with BH. Nevertheless, quality of image subtraction did not differ between techniques and non-diagnostic subtraction images occurred in only a minority of patients using NAV. Moreover, diagnostic accuracy for detection of enhancement in cystic and solid renal masses compared to non-enhancing cysts did not differ for either radiologist when using subjective assessment of BH and NAV subtraction images and was also comparable when using quantitative signal intensity measurements measured on both data sets. Our results suggest that free-breathing Navigator-triggered acquisitions of the kidneys are of sufficient quality to assess for enhancement in renal masses and may be particularly valuable in patients where breath-hold imaging may be limited.

In 1989, Ehman and Felmlee developed an adaptive Navigator technique where encoded "Navigator" echoes interleaved with the imaging sequence could be post-processed to provide a highly detailed record of the displacements and phase shifts that occur during imaging to improve images degraded by voluntary motion [28, 31, 32]. Free-breathing techniques have since then been expanded with various modifications [20, 28, 32–38] for abdominal MRI. Free-breathing techniques have now been employed in a variety of imaging fields, including thoracic, cardiac, pediatric, and hepatic imaging [28, 39, 40]. To our knowledge, this is the first study to apply a free-breathing T1W sequence in renal imaging for the purpose of obtaining subtraction image sets to assess for enhancement in cystic and solid masses.

Previous studies assessing T1W free-breathing sequences in adult abdominal imaging using radial data sampling [36] and pediatric abdominal imaging with Navigator acquisitions [28] demonstrated similar results to our study with a decrease in overall image quality comparing the free-breathing sequences to conventional breath-hold imaging. In a study by Reiner et al which only studied the subset of patients who were unable to breath-hold, radial T1W free-breathing sequences were actually shown to have superior image quality and anatomic conspicuity compared to breath-hold imaging [41]. Similarly, when assessing high-resolution T2W Navigator sequences in the liver, Lee et al demonstrated that the Navigator sequence improved the detectability of focal hepatic lesions with better image sharpness and higher lesion-to-liver contrast of solid lesions compared to the breath-hold sequences [42]. Their results may be partially explained by the higher spatial resolution which can be obtained with free-breathing imaging techniques which are not restricted by the need to minimize phase encoding to keep breath-hold lengths reasonably short. Free-breathing techniques have also been applied to pancreatic and gastric imaging with similar results [40, 43].

Table 5 Sensitivity, specificity, and area under the receiver operator characteristic (ROC) curve for detection of enhancement in benign renal cysts and cystic or solid renal masses using percentage signal intensity change as measured on breath-hold and free-breathing Navigator-triggered pre- and post-gadolinium-enhanced 3-D T1W FS GRE

	Sensitivity (confidence intervals)	Specificity (confidence intervals)	Area under ROC curve (standard error)	*p* value[1]
Breath-hold	70.6 (52.5–84.9)	81.7 (70.7–89.9)	0.76 (0.05)	0.74
Free-breathing navigator	73.5 (55.6–87.1)	76.1 (64.5–85.4)	0.75 (0.05)	

Percentage signal intensity change = ([signal intensity on post-gadolinium-enhanced signal intensity on pre-gadolinium enhanced])/signal intensity on pre-gadolinium enhanced)*100. A threshold of > 15% signal intensity change was used to define enhancement as suggested in the study by Ho et al [17]

[1] Comparisons were performed between groups using ROC statistic

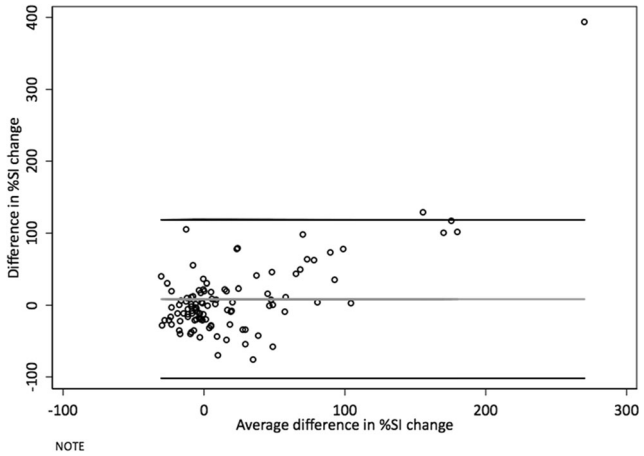

Fig. 5 A Bland-Altman plot depicting agreement in measurements of enhancement using quantitative percentage signal intensity change comparing breath-hold and Navigator-triggered LAVA

Enhancement of renal masses, evaluated by MRI, can be performed subjectively using subtraction images or quantitatively. The limitation of subtraction imaging is that it requires perfectly co-registered data, which is not always possible in patients who are unable to breath-hold. When judging enhancement of cystic and solid renal masses with subtraction imaging, we found a similar sensitivity and specificity compared to the previous seminal paper by Hecht [18], with a high sensitivity but lower specificity. In our study, there was no difference comparing qualitative assessment of enhancement using subtraction images from BH and NAV for both radiologists. Our quantitative results also demonstrated no difference when determining enhancement comparing BH and NAV acquisitions with a high degree of accuracy in measurements. Compared to subjective evaluation, enhancement judged quantitatively showed slightly improved sensitivity with lower specificity and no difference in overall accuracy. This is in contrast to the prior study by Hecht et al where qualitative assessment was more sensitive and more specific compared to quantitative analysis, however, without a statistically significant difference between the two techniques [18]. The differences may relate to a smaller proportion of intrinsically T1W hyperintense renal lesions in our study.

When compared to conventional BH imaging, NAV imaging has a longer acquisition time; this temporal trade-off occurs because a majority of data with NAV will occur outside the preselected limits of diaphragmatic excursion and will be rejected [28]. These temporal differences impose limitations in the application of NAV as a replacement for BH in the dynamic gadolinium-enhanced acquisition of the kidneys; however, it could be used as a rescue sequence in patients who are not able to BH effectively. With advances in parallel and keyhole imaging techniques, investigators have begun to introduce NAV acquisitions as free-breathing methods to dynamically assess the abdomen with gadolinium-enhanced MRI with promising early results; however, these will require further study [44]. As discussed, an alternative to the NAV free-breathing solution to abdominal MRI is a radial data sampling scheme which has also been combined with parallel imaging and keyhole imaging for free-breathing dynamic acquisitions of the abdomen [45, 46]. Radial and NAV T1W acquisitions are currently restricted to a particular vendor on clinical systems; therefore, comparing the two methods in the same patient cohort would require repeated examinations on two different clinical systems and therefore two injections of gadolinium. This is a challenge for head-to-head comparison of the two technologies; however, future studies are required to assess the ability of the radial sampling technique to generate subtraction imaging in renal MRI compared to the results using NAV in the present study. The strengths and limitations of NAV compared to radial sampling for motion correction in free-breathing abdominal MRI are beyond the scope of this manuscript; however, these have been discussed elsewhere [47]. Future studies comparing MR imaging sequences in renal MRI might also incorporate deep learning algorithms evaluating image quality, in addition to or potentially as a replacement of conventional interpretations by radiologists as has been described recently [48].

Our study has limitations. Our sample size is relatively small; however, since many patients had more than one renal lesion and assessment of enhancement (which was our primary outcome) was performed on a per-lesion basis, our sample of non-enhancing cysts and cystic and solid renal masses is robust. A limitation of performing per-lesion analysis in patients with multiple lesions is cluster bias, which impacts our reported results. Few of our renal masses had histological confirmation; this can be expected since benign cysts are diagnosed with a high degree of accuracy with imaging (not requiring histological confirmation) and because surveillance is now commonly performed for Bosniak IIF cysts and increasing in Bosniak III and solid renal masses measuring < 4 cm in size [6, 49–51]. The sensitivity for detection of enhancement in our study is lower than expected in renal MRI. Radiologists did not evaluate the other pre-contrast sequences or the raw data from the pre- and post-gadolinium-enhanced LAVA sequences when judging for the presence of enhancement. This study design, which undoubtedly lowered the reported sensitivity for enhancement, was selected in order to not bias interpretation of subtraction images. For example, in a hemorrhagic/proteinaceous cyst with marked homogeneous increased T1W signal intensity on pre-contrast LAVA sequences, a diagnosis can be made irrespective of findings on subtraction images [22, 23], which may have biased results. Similarly, the presence of internal septae in cystic masses detected on T2W images may have biased a radiologist towards detecting the presence of enhancing septae on motion-degraded images. Though our methodology underestimates the sensitivity of renal MRI for detection of enhancement in cystic and solid masses, it was in our opinion necessary to provide the fairest and most robust comparison of subtraction images. The difference in years

of experience of the two radiologists in our study can be considered a limitation; however, image quality scores and accuracy for determination of enhancement using BH and NAV were similar between the two radiologists which we feel further strengthens our study reproducibility since results were comparable in both an experienced and inexperienced user.

In conclusion, our study indicates that a free-breathing Navigator-triggered 3-D T1W GRE sequence in the abdomen can be used to generate high-quality pre- and post-gadolinium-enhanced image sets and subtraction images. Though overall image quality, image sharpness, and motion artifacts were better on breath-hold imaging, image subtraction and accuracy for detection of enhancement in cystic and solid renal masses judged subjectively on subtraction images and using quantitative signal intensity thresholds did not differ comparing the two imaging techniques. Free-breathing Navigator-triggered 3-D T1W GRE (and potentially other free-breathing abdominal MRI techniques) may offer an alternative for renal MRI in patients who cannot comply with breath-hold instructions required to generate high-quality subtraction images of the kidneys.

Funding The authors state that this work has not received any funding.

Compliance with ethical standards

Guarantor The scientific guarantor of this publication is Nicola Schieda, MD.

Conflict of interest The authors of this manuscript declare no relationships with any companies, whose products or services may be related to the subject matter of the article.

Statistics and biometry One of the authors has significant statistical expertise: Nicola Schieda, the Ottawa Hospital -University of Ottawa, corresponding author.

Informed consent Written informed consent was waived by the institutional review board.

Ethical approval Institutional review board approval was waived under a quality assurance waiver.

Methodology
- Retrospective
- Cross-sectional study
- Performed at one institution

References

1. Heilbrun ME, Remer EM, Casalino DD et al (2015) ACR Appropriateness Criteria indeterminate renal mass. J Am Coll Radiol 12:333–341
2. Krishna S, Murray CA, McInnes MD et al (2017) CT imaging of solid renal masses: pitfalls and solutions. Clin Radiol 72:708–721
3. Ramamurthy NK, Moosavi B, McInnes MD, Flood TA, Schieda N (2014) Multiparametric MRI of solid renal masses: pearls and pitfalls. Clin Radiol. https://doi.org/10.1016/j.crad.2014.10.006
4. Israel GM, Bosniak MA (2005) How I do it: evaluating renal masses. Radiology 236:441–450
5. Bosniak MA (1986) The current radiological approach to renal cysts. Radiology 158:1–10
6. Bosniak MA (2012) The Bosniak renal cyst classification: 25 years later. Radiology 262:781–785
7. Dilauro M, Quon M, McInnes MD et al (2016) Comparison of contrast-enhanced multiphase renal protocol CT versus MRI for diagnosis of papillary renal cell carcinoma. AJR Am J Roentgenol 206: 319–325
8. Egbert ND, Caoili EM, Cohan RH et al (2013) Differentiation of papillary renal cell carcinoma subtypes on CT and MRI. AJR Am J Roentgenol 201:347–355
9. Israel GM, Bosniak MA (2008) Pitfalls in renal mass evaluation and how to avoid them. Radiographics 28:1325–1338
10. Siddaiah M, Krishna S, McInnes MDF et al (2017) Is ultrasound useful for further evaluation of homogeneously hyperattenuating renal lesions detected on CT? AJR Am J Roentgenol 209:604–610
11. Schieda N, Dilauro M, Moosavi B et al (2015) MRI evaluation of small (<4cm) solid renal masses: multivariate modeling improves diagnostic accuracy for angiomyolipoma without visible fat compared to univariate analysis. Eur Radiol. https://doi.org/10.1007/s00330-015-4039-y
12. Canvasser NE, Kay FU, Xi Y et al (2017) Diagnostic accuracy of multiparametric magnetic resonance imaging to identify clear cell renal cell carcinoma in cT1a renal masses. J Urol 198:780–786
13. Cornelis F, Tricaud E, Lasserre AS et al (2014) Routinely performed multiparametric magnetic resonance imaging helps to differentiate common subtypes of renal tumours. Eur Radiol 24:1068–1080
14. Cornelis F, Grenier N (2017) Multiparametric magnetic resonance imaging of solid renal tumors: a practical algorithm. Semin Ultrasound CT MR 38:47–58
15. Willatt JM, Hussain HK, Chong S et al (2014) MR imaging in the characterization of small renal masses. Abdom Imaging 39:761–769
16. Ramamurthy NK, Moosavi B, McInnes MD, Flood TA, Schieda N (2015) Multi-parametric (MP) MRI of solid renal masses: pearls and pitfalls. Clin Radiol. https://www.ncbi.nlm.nih.gov/pubmed/25472466
17. Ho VB, Allen SF, Hood MN, Choyke PL (2002) Renal masses: quantitative assessment of enhancement with dynamic MR imaging. Radiology 224:695–700
18. Hecht EM, Israel GM, Krinsky GA et al (2004) Renal masses: quantitative analysis of enhancement with signal intensity measurements versus qualitative analysis of enhancement with image subtraction for diagnosing malignancy at MR imaging. Radiology 232:373–378
19. Kim KW, Lee JM, Jeon YS et al (2013) Free-breathing dynamic contrast-enhanced MRI of the abdomen and chest using a radial gradient echo sequence with K-space weighted image contrast (KWIC). Eur Radiol 23:1352–1360
20. Chandarana H, Block KT, Winfeld MJ et al (2014) Free-breathing contrast-enhanced T1-weighted gradient-echo imaging with radial k-space sampling for paediatric abdominopelvic MRI. Eur Radiol 24:320–326
21. O'Connor SD, Silverman SG, Ip IK, Maehara CK, Khorasani R (2013) Simple cyst-appearing renal masses at unenhanced CT: can they be presumed to be benign? Radiology 269:793–800
22. Davarpanah AH, Spektor M, Mathur M, Israel GM (2016) Homogeneous T1 Hyperintense renal lesions with smooth borders: is contrast-enhanced MR imaging needed? Radiology 281:326
23. Kim CW, Shanbhogue KP, Schreiber-Zinaman J, Deng FM, Rosenkrantz AB (2017) Visual assessment of the intensity and pattern of T1 Hyperintensity on MRI to differentiate hemorrhagic renal cysts from renal cell carcinoma. AJR Am J Roentgenol 208:337–342

24. Jonisch AI, Rubinowitz AN, Mutalik PG, Israel GM (2007) Can high-attenuation renal cysts be differentiated from renal cell carcinoma at unenhanced CT? Radiology 243:445–450
25. Israel GM, Hindman N, Bosniak MA (2004) Evaluation of cystic renal masses: comparison of CT and MR imaging by using the Bosniak classification system. Radiology 231:365–371
26. Schieda N, Avruch L, Flood TA (2014) Small (<1 cm) incidental echogenic renal cortical nodules: chemical shift MRI outperforms CT for confirmatory diagnosis of angiomyolipoma (AML). Insights Imaging. https://doi.org/10.1007/s13244-014-0323-7
27. Schieda N, Hodgdon T, El-Khodary M, Flood TA, McInnes MD (2014) Unenhanced CT for the diagnosis of minimal-fat renal angiomyolipoma. AJR Am J Roentgenol 203:1236–1241
28. Vasanawala SS, Iwadate Y, Church DG, Herfkens RJ, Brau AC (2010) Navigated abdominal T1-W MRI permits free-breathing image acquisition with less motion artifact. Pediatr Radiol 40:340–344
29. Samji K, Alrashed A, Shabana WM, McInnes MD, Bayram E, Schieda N (2016) Comparison of high-resolution T1W 3D GRE (LAVA) with 2-point Dixon fat/water separation (FLEX) to T1W fast spin echo (FSE) in prostate cancer (PCa). Clin Imaging 40:407–413
30. Schieda N, Avruch L, Shabana WM, Malone SC (2015) Multi-echo gradient recalled echo imaging of the pelvis for improved depiction of brachytherapy seeds and fiducial markers facilitating radiotherapy planning and treatment of prostatic carcinoma. J Magn Reson Imaging 41:715–720
31. Ehman RL, Felmlee JP (1989) Adaptive technique for high-definition MR imaging of moving structures. Radiology 173:255–263
32. Klessen C, Asbach P, Kroencke TJ et al (2005) Magnetic resonance imaging of the upper abdomen using a free-breathing T2-weighted turbo spin echo sequence with navigator triggered prospective acquisition correction. J Magn Reson Imaging 21:576–582
33. Tyszka JM, Silverman JM (1998) Navigated single-voxel proton spectroscopy of the human liver. Magn Reson Med 39:1–5
34. Tokuda Y, Kuriyama K, Nakamoto A et al (2009) Evaluation of suspicious nipple discharge by magnetic resonance mammography based on breast imaging reporting and data system magnetic resonance imaging descriptors. J Comput Assist Tomogr 33:58–62
35. Kim ID, Azuma T, Ido A et al (2006) Navigator-echo-based MR provides high-resolution images and precise volumetry of swine livers without breath holding or injection of contrast media. Liver Transpl 12:72–77
36. Azevedo RM, de Campos RO, Ramalho M, Herédia V, Dale BM, Semelka RC (2011) Free-breathing 3D T1-weighted gradient-echo sequence with radial data sampling in abdominal MRI: preliminary observations. AJR Am J Roentgenol 197:650–657
37. Seo N, Park SJ, Kim B et al (2016) Feasibility of free-breathing dynamic contrast-enhanced MRI of the abdomen: a comparison between CAIPIRINHA-VIBE, Radial-VIBE with KWIC reconstruction and conventional VIBE. Br J Radiol 89:20160150
38. Chu ML, Chang HC, Chung HW et al (2018) Free-breathing abdominal MRI improved by repeated k-t-subsampling and artifact-minimization (ReKAM). Med Phys 45:178–190
39. Spuentrup E, Katoh M, Buecker A et al (2004) Free-breathing 3D steady-state free precession coronary MR angiography with radial k-space sampling: comparison with cartesian k-space sampling and cartesian gradient-echo coronary MR angiography–pilot study. Radiology 231:581–586
40. Bamrungchart S, Tantaway EM, Midia EC et al (2013) Free breathing three-dimensional gradient echo-sequence with radial data sampling (radial 3D-GRE) examination of the pancreas: comparison with standard 3D-GRE volumetric interpolated breathhold examination (VIBE). J Magn Reson Imaging 38:1572–1577
41. Reiner CS, Neville AM, Nazeer HK et al (2013) Contrast-enhanced free-breathing 3D T1-weighted gradient-echo sequence for hepatobiliary MRI in patients with breath-holding difficulties. Eur Radiol 23:3087–3093
42. Lee SS, Byun JH, Hong HS et al (2007) Image quality and focal lesion detection on T2-weighted MR imaging of the liver: comparison of two high-resolution free-breathing imaging techniques with two breath-hold imaging techniques. J Magn Reson Imaging 26:323–330
43. Li HH, Zhu H, Yue L et al (2018) Feasibility of free-breathing dynamic contrast-enhanced MRI of gastric cancer using a golden-angle radial stack-of-stars VIBE sequence: comparison with the conventional contrast-enhanced breath-hold 3D VIBE sequence. Eur Radiol 28:1891–1899
44. Boss A, Schaefer JF, Martirosian P et al (2006) Contrast-enhanced dynamic MR nephrography using the TurboFLASH navigator-gating technique in children. Eur Radiol 16:1509–1518
45. Riffel P, Zoellner FG, Budjan J et al (2016) "One-stop shop": free-breathing dynamic contrast-enhanced magnetic resonance imaging of the kidney using iterative reconstruction and continuous golden-angle radial sampling. Invest Radiol 51:714–719
46. Chandarana H, Feng L, Block TK et al (2013) Free-breathing contrast-enhanced multiphase MRI of the liver using a combination of compressed sensing, parallel imaging, and golden-angle radial sampling. Invest Radiol 48:10–16
47. Stehning C (2005) Motion correction and volumetric acquisition techniques for coronary magnetic resonance angiography. https://books.google.ca/books/about/Motion_Correction_and_Volumetric_Acquisi.html?id=HRF6HAAACAAJ&redir_esc=y. Accessed 12 May 2018
48. Esses SJ, Lu X, Zhao T et al (2018) Automated image quality evaluation of T2 -weighted liver MRI utilizing deep learning architecture. J Magn Reson Imaging 47:723–728
49. Ng CS, Wood CG, Silverman PM, Tannir NM, Tamboli P, Sandler CM (2008) Renal cell carcinoma: diagnosis, staging, and surveillance. AJR Am J Roentgenol 191:1220–1232
50. Pierorazio PM, Hyams ES, Mullins JK, Allaf ME (2012) Active surveillance for small renal masses. Rev Urol 14:13–19
51. Smaldone MC, Kutikov A, Egleston BL et al (2012) Small renal masses progressing to metastases under active surveillance: a systematic review and pooled analysis. Cancer 118:997–1006